Electrochemistry of Multicomponent Systems. Redox Series Comprising up to 26 Reversible Reduction Processes in Polynuclear Ruthenium(II) Bipyridine-Type Complexes

Massimo Marcaccio,[†] Francesco Paolucci,[†] Carmen Paradisi,[†] Sergio Roffia,*,[†,‡] Claudio Fontanesi,[§] Lesley J. Yellowlees,[⊥] Scolastica Serroni,[||] Sebastiano Campagna,[||] Gianfranco Denti,[▽] and Vincenzo Balzani*,[†,○]

Contribution from the Dipartimento di Chimica "G. Ciamician", Università di Bologna, Via Selmi 2, 40126 Bologna, Italy, Dipartimento di Chimica, Università di Modena, via Campi 183, 41100 Modena, Italy, Department of Chemistry, University of Edinburgh, King's Buildings, West Mains Road, Edinburgh EH9 3JJ, U.K., Dipartimento di Chimica Inorganica, Chimica Analitica e Chimica Fisica, Università di Messina, via Sperone 31, 98166 Messina, Italy, and Dipartimento di Chimica e Biotecnologie Agrarie, Università di Pisa, via del Borghetto 80, 56124 Pisa, Italy

Received May 17, 1999

Abstract: The electrochemical behavior of a family of polynuclear ruthenium(II) bipyridine-type complexes with 2,3-bis(2-pyridyl)pyrazine (2,3-dpp) and 2,5-bis(2-pyridyl)pyrazine (2,5-dpp) as bridging ligands has been investigated in highly purified *N,N*-dimethylformamide solution. The compounds studied contain two, three, four, and six metal centers and have general formula $[Ru_n(bpy)_{n+2}(2,X\text{-dpp})_{n-1}]^{2n+}$, where $n = 2, 3, 4,$ or 6, $X = 3$ or 5, and bpy is 2,2′-bipyridine. The wide cathodic potential window explored (up to ca. −3.1 V vs SCE) has allowed us to observe the most extensive ligand-centered redox series so far reported, comprising up to 26 reversible reduction processes for the hexanuclear complex. The redox standard potentials for overlapping processes in multielectron waves have been obtained from the analysis of the voltammetric curves and their digital simulation. The localization of each redox process and the mutual interactions of the redox centers have been elucidated through the analysis and comparison of the redox series of the various compounds. For the dinuclear species, the assignment of the redox sites has been confirmed by semiempirical molecular orbital calculations (ZINDO) and spectroelectrochemical experiments. Calculations also substantiate the important role played by bridging ligands in mediating the interactions between equivalent redox sites. Finally, it has been shown that the size of the supporting electrolyte cation has an influence on the processes occurring at the extreme cathodic region.

Introduction

The wide interest in the study of the electrochemical properties of multicomponent systems[1] stems from their potential use for designing new materials and devices. Ruthenium(II) bipyridine-type complexes[2] are suitable building blocks to construct multicomponent systems capable of exhibiting inter-

esting electrochemical, photochemical, and photophysical properties.[3]

In the past few years a great number of polynuclear ruthenium(II) bipyridine-type complexes have been synthesized.[4] A particularly interesting family of polynuclear Ru(II) complexes is that based on the 2,3-bis(2-pyridyl)pyrazine (2,3-dpp) and 2,5-bis(2-pyridyl)pyrazine (2,5-dpp) bridging ligands. Using the so-called complexes-as-metals and complexes-as-ligands synthetic strategy,[5] branched polynuclear Ru(II) species of general formula $[Ru_n(bpy)_{n+2}(2,X\text{-dpp})_{n-1}]^{2n+}$, where $n = 2, 3, 4,$ or 6, $X = 3$ or 5, and bpy is 2,2′-bipyridine, containing up to 22 metal centers, 21 bridging ligands, and 24 terminal ligands have been obtained.[6] The photophysical properties of these

[†] Università di Bologna.
[‡] E-mail: Roffia@ciam.unibo.it. Fax: +39 051 2099456.
[§] Università di Modena.
[⊥] University of Edinburgh.
[||] Università di Messina.
[▽] Università di Pisa.
[○] E-mail: VBalzani@ciam.unibo.it. Fax: +39 051 2099456.
(1) (a) Ammar, F.; Savéant, J. M. *J. Electroanal. Chem.* **1973,** *47,* 115. (b) Flanagan, J. B.; Margel, A.; Bard, A. J.; Anson, F. C. *J. Am. Chem. Soc.* **1978,** *100,* 4248. (c) Bard, A. J. *Integrated Chemical Systems*; Wiley: New York, 1994. (d) Bryce, M. R.; Devonport, W. In *Advances in Dendritic Macromolecules*; Newkome, G. R., Ed.; JAY Press: London, 1996; Vol. 3, p 115. (e) Kaifer, A.; Mendoza, S. In *Comprehensive Supramolecular Chemistry*; Atwood, J. L., Davies, J. E. D., MacNicol, D. D., Vögtle, F., Eds.; Pergamon: Oxford, 1996; Vol. 1, p 701. (f) Astruc, D. *Acc. Chem. Res.* **1997,** *30,* 383. (g) Gorman, C. B. *Adv. Mater.* **1997,** *9,* 1117. (h) Boulas, P. L.; Gomez-Kaifer, M.; Echegoyen, L. *Angew. Chem., Int. Ed.* **1998,** *37,* 216.
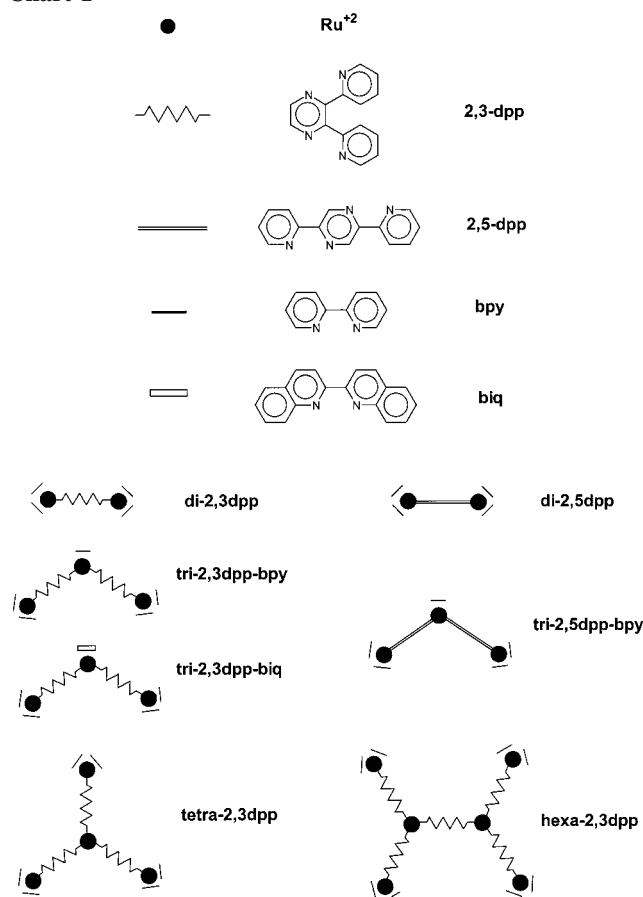(2) (a) Juris, A.; Balzani, V.; Barigelletti, F.; Campagna, S.; Belser, P.; von Zelewsky, A. *Coord. Chem. Rev.* **1988,** *84,* 85. (b) Meyer, T. J. *Acc. Chem. Res.* **1989,** *22,* 163. (c) Kalyanasundaram, K. *Photochemistry of Polypyridine and Porphyrin Complexes*; Academic Press: London, 1991.

(3) (a) Balzani, V.; Scandola, F. *Supramolecular Photochemistry*; Horwood: Chichester, 1991. (b) O'Regan, B.; Graetzel, M. *Nature* **1991,** *353,* 737. (c) Graetzel, M. *Comments Inorg. Chem.* **1991,** *12,* 93. (d) Keller, S. W.; Johnson, S. A.; Brigham, E. S.; Yonemoto, E. T.; Mallouk, T. E. *J. Am. Chem. Soc.* **1995,** *117,* 12879. (e) Cusack, L.; Rao, S. N.; Fitzmaurice, D. *Chem. Eur. J.* **1997,** *3,* 202. (f) Bignozzi, C. A.; Scandola, F.; Schoonover, J. R. *Prog. Inorg. Chem.* **1997,** *44,* 1. (g) Dupray, L. M.; Devenney, M.; Striplin, D. R.; Meyer, T. J. *J. Am. Chem. Soc.* **1997,** *119,* 10243.
(4) Balzani, V.; Juris, A.; Venturi, M.; Campagna, S.; Serroni, S. *Chem. Rev.* **1996,** *96,* 759.
(5) (a) Campagna, S.; Denti, G.; Serroni, S.; Ciano, M.; Balzani, V. *Inorg. Chem.* **1991,** *30,* 3728. (b) Denti, G.; Serroni, S.; Campagna, S.; Juris, A.; Ciano, M.; Balzani, V. In *Perspectives in Coordination Chemistry*; Williams, A. F., Floriani, C., Merbach, A. E., Eds.; VCH: Basel, 1992; p 153.

Chart 1

Ru^{+2}

2,3-dpp

2,5-dpp

bpy

biq

di-2,3dpp

di-2,5dpp

tri-2,3dpp-bpy

tri-2,5dpp-bpy

tri-2,3dpp-biq

tetra-2,3dpp

hexa-2,3dpp

complexes have been carefully studied in relation to the design of light-harvesting dendrimers,[6,7] and their electrochemical behavior has also been investigated although in a limited potential window.[6,8]

In this paper we have thoroughly investigated the electrochemical reduction processes of some of these polynuclear complexes, devoting particular attention to obtain highly aprotic experimental conditions to extend the useful potential window (up to ca. −3.1 V vs SCE) and to eliminate any nonintrinsic reactivity of the generated electrodic species.[9] All the compounds studied are shown in Chart 1. The experimental conditions used have allowed us to observe the most extensive ligand-centered redox series so far reported, comprising up to 26 reversible reduction processes for the hexanuclear complex. We have also investigated the localization of the redox processes and the mutual interactions of the redox centers. Semiempirical molecular orbital calculations (ZINDO) and spectroelectrochemical experiments have been used to confirm the assignment of the redox sites. Finally, we have found that the size of the electrolyte cation plays an important role in the processes occurring at the extreme cathodic region.

Experimental Section

The ligands 2,3-bis(2-pyridyl)pyrazine (2,3-dpp)[10] and 2,5-bis(2-pyridyl)pyrazine (2,5-dpp)[11] were prepared according to literature

methods. All the polynuclear complexes studied were prepared according to previously described methods.[4,12]

Tetraethylammonium tetrafluoroborate (TEATFB) and tetrabutylammonium tetrafluoroborate (TBATFB) from Fluka were used as supporting electrolyte as received. Dry vacuum-distilled *N,N*-dimethylformamide (DMF) was purified using sodium anthracenide to remove any traces of water and oxygen, according to the method of Aoyagui and co-workers.[13] Acetonitrile, after being refluxed over CaH$_2$, was distilled under vacuum at room temperature with a high refluxing ratio, utilizing a 1 m length distillation column filled with glass rings, and it was stored in a specially designed Schlenk flask over 3 Å activated molecular sieves, protected from light.

The solvent, purified as described above, was distilled via a closed system into an electrochemical cell containing the supporting electrolyte and the species under examination, just before the experiment was performed. All the other chemicals were of reagent grade.

Electrochemical experiments were carried out in an air-tight single-compartment cell described elsewhere,[14] by using platinum as working and counter electrodes and a silver spiral as a quasi-reference electrode. The drift of the quasi-reference electrode was negligible for the time required by an experiment.

The $E_{1/2}$ values have been determined by averaging the anodic and cathodic peak potentials for those processes which are well separated from each other, while by simulation of the voltammetric curves for those processes overlapping in a single voltammetric wave with potential separation less than about 50 mV. Digital simulation of the voltammetric curves has been carried out using DigiSim 2.1 software (by Bioanalytical System Inc.) and considering all the processes as electrochemically and chemically reversible. All the $E_{1/2}$ potentials are referred to an aqueous saturated calomel electrode (SCE). The $E_{1/2}$ values have been determined by adding, at the end of each experiment, ferrocene as an internal standard,[15] and measuring them with respect to the ferrocinium/ferrocene couple standard potential.

The cell containing the supporting electrolyte and the electroactive compound was dried under vacuum at 110−120 °C for at least 60 h before each experiment. The pressure measured in the electrochemical cell prior to the trap-to-trap distillation of the solvent being performed was typically $(1-2) \times 10^{-5}$ mbar.

Voltammograms were recorded with an AMEL Model 552 potentiostat controlled by an AMEL Model 568 programmable function generator, an AMEL Model 865 A/D converter, a Hewlett-Packard 7475A digital plotter, and a Nicolet Model 3091 digital oscilloscope. The minimization of the uncompensated resistance effect in the voltammetric measurements was achieved by the positive-feedback circuit of the potentiostat. For differential pulse voltammetry experiments, the equipment used was an AMEL Model 466 polarographic analyzer.

The spectroelectrochemical experiments have been carried out using a quartz OTTLE cell with a 0.03 cm path length. Temperature control was achieved by a special cell holder with quartz windows and two nitrogen fluxes (one at room temperature and the other at low temperature), regulated by two needle valves. All the spectra have been recorded by a Perkin-Elmer Lambda-9 and a Perkin-Elmer Model PP-1 plotter printer. All the experimental details for the spectroelectrochemical setup have been reported elsewhere.[16]

(6) (a) Campagna, S.; Denti, G.; Serroni, S.; Juris, A.; Venturi, M.; Ricevuto, V.; Balzani, V. *Chem. Eur. J.* **1995**, *1*, 211. (b) Serroni, S.; Juris, A.; Venturi, M.; Campagna, S.; Resino, I. R.; Denti, G.; Credi, A.; Balzani, V. *J. Mater. Chem.* **1997**, *7*, 1227 and references therein.

(7) Balzani, V.; Campagna, S.; Denti, G.; Juris, A.; Serroni, S.; Venturi, M. *Acc. Chem. Res.* **1998**, *31*, 26.

(8) Venturi, M.; Serroni, S.; Juris, A.; Campagna, S.; Balzani, V. *Top. Curr. Chem.* **1998**, *197*, 193.

(9) (a) Maloy, J. T.; Prater, K. B.; Bard, A. J. *J. Am. Chem. Soc.* **1971**, *93*, 5959. (b) Heinze, J. *Angew. Chem., Int. Ed. Engl.* **1984**, *23*, 831.

(10) Goodwin, H. A.; Lions, F. *J. Am. Chem. Soc.* **1959**, *81*, 6415.

(11) Case, F. H.; Koft, E. *J. Am. Chem. Soc.* **1959**, *81*, 905.

(12) Denti, G.; Campagna, S.; Sabatino, L.; Serroni, S.; Ciano, M.; Balzani, V. *Inorg. Chem.* **1990**, *29*, 4750.

(13) Saji, T.; Yamada, T.; Aoyagui, S. *J. Electroanal. Chem.* **1975**, *61*, 147.

(14) (a) Paolucci, F.; Marcaccio, M.; Roffia, S.; Orlandi, G.; Zerbetto, F.; Prato, M.; Maggini, M.; Scorrano, G. *J. Am. Chem. Soc.* **1995**, *117*, 6572. (b) Paolucci, F.; Marcaccio, M.; Paradisi, C.; Roffia, S.; Bignozzi, C. A.; Amatore, A. *J. Phys. Chem. B* **1998**, *102*, 4759.

(15) Kuwana, T.; Bublitz, D. E.; Hoh, G. J. *J. Am. Chem. Soc.* **1960**, *82*, 5811.

(16) (a) MacGregor, S. A.; McInnes, E.; Sorbie, R. J.; Yellowlees, L. J. In *Molecular Electrochemistry of Inorganic, Bioinorganic and Organometallic Compounds*; Pombeiro, A. J. L., McCleverty, J. A., Eds.; Kluwer Academic Publishers: Dordrecht, The Netherlands, 1993; Vol. 385, p 503. (b) Lee, S.-M.; Kowallick, R.; Marcaccio, M.; McCleverty, J. A.; Ward, M. D. *J. Chem. Soc., Dalton Trans.* **1998**, 3443.
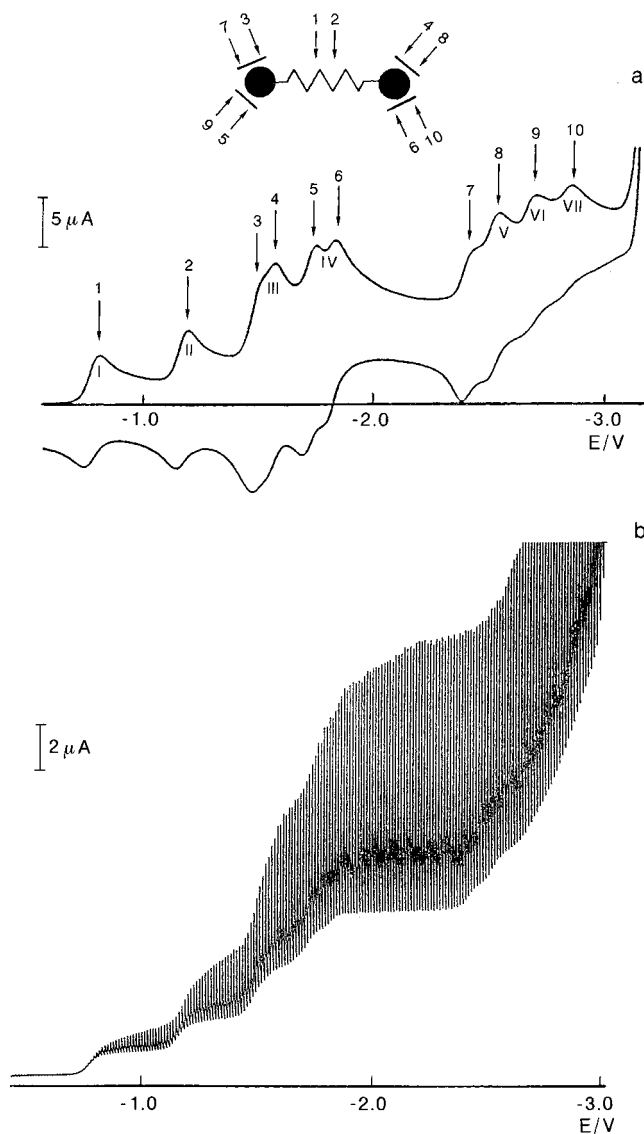
Figure 1. (a) Cyclic voltammetric curve for a 0.5 mM [(bpy)$_2$Ru(2,3-dpp)Ru(bpy)$_2$]$^{4+}$, 0.05 M TEATFB/DMF solution. Working electrode Pt; $T = -54$ °C; scan rate 0.1 V/s. The proposed localization of the redox processes is indicated. (b) Voltammetric curve recorded with a Pt electrode with a periodical renewal of the diffusion layer for a 0.5 mM [(bpy)$_2$Ru(2,3-dpp)Ru(bpy)$_2$]$^{4+}$, 0.05 M TEATFB/DMF solution. $T = -54$ °C; renewal time 3 s.

Figure 2. (a) Cyclic voltammetric curve for a 0.5 mM [(bpy)$_2$Ru(2,5-dpp)Ru(bpy)$_2$]$^{4+}$, 0.05 M TEATFB/DMF solution. Working electrode Pt; $T = -54$ °C; scan rate 0.1 V/s. The proposed localization of the redox processes is indicated. (b) Voltammetric curve recorded with a Pt electrode with a periodical renewal of the diffusion layer for a 0.5 mM [(bpy)$_2$Ru(2,5-dpp)Ru(bpy)$_2$]$^{4+}$, 0.05 M TEATFB/DMF solution. $T = -54$ °C; renewal time 3 s.

Results and Discussion

Dinuclear Complexes. The dinuclear species [(bpy)$_2$Ru(2,3-dpp)Ru(bpy)$_2$]$^{4+}$ and [(bpy)$_2$Ru(2,5-dpp)Ru(bpy)$_2$]$^{4+}$, which contain a relatively small number of redox centers, can be considered as model compounds to understand the electrochemistry of the complexes of higher nuclearity. In the dinuclear species, the knowledge of the voltammetric behavior of the mononuclear building blocks and the comparison of the redox series relative to the two species have allowed us to establish the localization for each redox process and to evaluate the mutual interactions existing between the redox sites.

The cyclic voltammetric curves (cvc's) recorded at a sweep rate of 0.1 V/s of the two dinuclear species [(bpy)$_2$Ru(2,3-dpp)Ru(bpy)$_2$]$^{4+}$ and [(bpy)$_2$Ru(2,5-dpp)Ru(bpy)$_2$]$^{4+}$ are shown in Figures 1a and 2a. In the available potential window (up to ~-3.1 V vs SCE, under the experimental conditions used) it is possible to observe seven and six voltammetric peaks for [(bpy)$_2$Ru(2,3-dpp)Ru(bpy)$_2$]$^{4+}$ and [(bpy)$_2$Ru(2,5-dpp)-

Ru(bpy)$_2$]$^{4+}$, respectively. Labeling the peaks by Roman numbers, we can see that, for both complexes, the first two peaks (I and II) correspond to one-electron processes, whereas the next three peaks (III, IV, and V) contain two closely spaced one-electron processes each. The remaining two redox processes of the redox series give rise to a two-electron voltammetric peak (VI) in the case of [(bpy)$_2$Ru(2,5-dpp)Ru(bpy)$_2$]$^{4+}$ species, and to a couple of one-electron peaks (VI and VII) for [(bpy)$_2$-Ru(2,3-dpp)Ru(bpy)$_2$]$^{4+}$. Ten successive one-electron reversible and diffusion-controlled reduction processes are then observed for both species, whose $E_{1/2}$ values, also obtained by digital simulation of the cvc's, are collected in Table 1. By examining the cvc's of the two complexes in Figures 1a and 2a, a remarkable resemblance between the two voltammetric patterns is observed, apart from a different separation between the processes within the two-electron peaks.

For both complexes the number of electrons exchanged in

Table 1. $E_{1/2}$ Values for the Electrodic Processes (V vs SCE)[a]

	I	II	III	IV	V	VI	VII
di-2,3dpp	−0.78	−1.17	−1.46	−1.70	−2.40	−2.66	−2.83
			−1.55	−1.82	−2.51		
di-2,5dpp	−0.66	−1.11	−1.50	−1.74	−2.43	−2.70	
			−1.55	−1.82	−2.51	−2.81	
tri-2,3dpp-bpy	−0.72	−1.15	−1.49	−1.67	−2.37	−2.69	
	−0.81	−1.26	−1.55	−1.76	−2.46	−2.78	
				−1.85	−2.55		
tri-2,5dpp-bpy	−0.61	−1.12	−1.50	−1.74	−2.44	−2.72	
	−0.71	−1.24	−1.56	−1.80	−2.49	−2.79	
				−1.87	−2.57		
tetra-2,3dpp	−0.64	−1.14	−1.45	−1.69	−2.41	−2.63	
	−0.73	−1.22	−1.52	−1.76	−2.45	−2.71	
	−0.82	−1.32	−1.57	−1.82	−2.50	−2.78	
hexa-2,3dpp	−0.65	−1.07	−1.40	−1.67	−2.42	−2.68	
	−0.70	−1.14	−1.44	−1.71	−2.46	−2.73	
	−0.76	−1.20	−1.48	−1.76	−2.50	−2.77	
	−0.81	−1.27	−1.52	−1.81	−2.54	−2.82	
		−1.32	−1.57				

[a] For the abbreviations used to indicate the compounds, see Chart 1. DMF solution, $T = -54\ °C$. In the case of multicomponent peaks, the $E_{1/2}$ values were obtained by digital simulation of the cvc's. The assignments of the observed processes are shown in the figures reporting the cvc's.

each voltammetric peak is in agreement with the results of both voltammetry with periodical renewal of the diffusion layer[17] and differential pulse voltammetry. In the case of [(bpy)$_2$-Ru(2,5-dpp)Ru(bpy)$_2$]$^{4+}$ the voltammetric curve at a Pt electrode with periodical renewal of the diffusion layer shows six waves whose heights are in the ratio 1:1:2:2:2:2 (Figure 2b). Similarly, the corresponding curve for the analogous [(bpy)$_2$Ru(2,3-dpp)-Ru(bpy)$_2$]$^{4+}$ complex, reported in Figure 1b, shows five waves with heights in the ratio 1:1:2:2:2. In the latter case the sixth wave is missing since the generated species in the extreme cathodic region are not stable enough to be observed.

Basically the same voltammetric pattern is observed in acetonitrile, with limited redox series only comprising those processes that occur within the narrower cathodic potential window of this solvent (∼−2.4 V). Contrary to what happens in DMF, severe adsorption phenomena occur in acetonitrile, especially at low temperature. A very strong, characteristic desorption peak arises upon reoxidation of the generated neutral species, i.e., on the anodic peak of the third two-electron voltammetric wave. This can be ascribed to the fact that acetonitrile is a worse solvent than DMF for neutral forms of this type of complex. Indeed, electrocrystallization of the neutral form of polypyridyl mononuclear Ru(II) complexes has been recently achieved in acetonitrile.[18]

To check a possible effect of the size of the electrolyte cation on the voltammetric pattern, the electrochemical investigation of these dinuclear species was also undertaken in DMF using a different base electrolyte, i.e., replacing the tetraethylammonium (TEA$^+$) tetrafluoborate electrolyte with tetrabutylammonium (TBA$^+$) tetrafluoborate. For both dinuclear complexes, the same voltammetric pattern and morphology were observed as for the first six redox processes, while, in the last part of the cvc's (beyond −2 V), only two one-electron peaks were observed when TBA$^+$ was used, instead of the four reductions observed with TEA$^+$. The observed effect is in agreement with the reported supporting electrolyte effect on the reduction $E_{1/2}$ values

of aromatic species, as a consequence of ion pair formation.[19] Since the cathodic processes for the present class of complexes are mainly ligand-centered, the effect can be attributed to the better ability of TEA$^+$ cations to give ion pairs with the electrogenerated anionic forms of the dinuclear species, thus stabilizing the elements of the redox series bearing the highest negative charges which are consequently anodically shifted.[20] In line with this explanation, while no significant change is observed for the first four one-electron redox steps, starting from the fifth one-electron process an increasing shift between the corresponding $E_{1/2}$ values is observed, the $E_{1/2}$ values in the TBA$^+$ solution being more cathodic than in the TEA$^+$ one. An expected value for the ninth reduction in TBA$^+$/DMF, based on an extrapolation of the plot of $\Delta E_{1/2}$ vs the total charge of the complex, is −3.08 V, just at the edge of the available potential window, which would explain why it is not detected.

Localization of Redox Sites and Their Mutual Interaction in Dinuclear Complexes. In this type of dendrimeric coordination compound the various subunits interact weakly with each other, so that a description of their redox properties in terms of the localized redox orbital model is possible.[2,4,7]

First of all, it should be noted that, on the basis of electrochemical studies carried out on the mononuclear building blocks of these polymetallic systems,[21,22] redox series made up of at least 12 and 10 one-electron reduction processes would be expected for the species with the 2,3-dpp and 2,5-dpp bridging ligand, respectively. Such an expectation is only fulfilled for [(bpy)$_2$Ru(2,5-dpp)Ru(bpy)$_2$]$^{4+}$, but not for the 2,3-dpp homologue since 10 redox processes are observed in both cases. The 2,3-dpp ligand was shown to undergo up to four reductions,[21] when it is coordinated to a Ru(II) center. Its bischelation to two metal centers should only move these reductions to less negative potentials, and a possible additional consequence of bischelation might be the increase of the number of bridge-centered redox processes (stabilization of a higher redox orbital) rather than its decrease, as experimentally observed. A possible explanation of these apparently contradictory findings is given below.

To identify the ligand-centered redox sites in the dinuclear complexes, we first take into account the different electrochemical behavior of the free ligands and the redox pattern of the mononuclear building blocks.[21,22] The redox series of the two dinuclear species, in which only the bridging ligand is different, will then be compared. Such a comparison is expected to show large differences in the peaks concerning the bridging ligand, while changes in the remaining part of the cvc's would evidence the different ability of the two isomeric bridging ligands in mediating the interaction between the terminal redox sites.

The electrochemical studies carried out on the free ligands bpy,[23] 2,3-dpp,[21] and 2,5-dpp[22] have established that the reduction potentials become more negative in going from 2,5-dpp to 2,3-dpp and finally to bpy. The same reduction order is observed in the Ru(II) mononuclear complexes.[21,22] These results, together with the strong stabilization of the molecular

(17) Farnia, G.; Roffia, S. *J. Electroanal. Chem.* **1981**, *122*, 347.

(18) (a) Perez-Cordero, E.; Buigas, R.; Brady, N.; Echegoyen, L.; Arana, C.; Lehn, J. M. *Helv. Chim. Acta* **1994**, *77*, 1222. (b) Perez-Cordero, E.; Brady, N.; Echegoyen, L.; Thummel, R.; Hung, C.-Y.; Bott, S. G. *Chem. Eur. J.* **1996**, *2*, 781.

(19) (a) Kalinowski, M. K. *Chem. Phys. Lett.* **1970**, *7*, 55. (b) Lasia, A. *J. Electroanal. Chem.* **1972**, *36*, 511. (c) Kapturkiewicz, A.; Opallo, M. *J. Electroanal. Chem.* **1985**, *185*, 15. (d) Fawcett, W. R.; Fedurco, M. *J. Phys. Chem.* **1993**, *97*, 7075.

(20) Takeko, M. I.; Tyuzu, I.; Masako, K.; Kiyo, K. *Nippon Kagaku Kaishi* **1982**, 72.

(21) Roffia, S.; Marcaccio, M.; Paradisi, C.; Paolucci, F.; Balzani, V.; Denti, G.; Serroni, S.; Campagna, S. *Inorg. Chem.* **1993**, *32*, 3003.

(22) Marcaccio, M.; Paolucci, F.; Paradisi, C.; Roffia, S.; Fontanesi, C.; Yellowlees, L. J.; Balzani, V.; Serroni, S.; Denti, G.; Campagna, S. To be published.

(23) Roffia, S.; Casadei, R.; Paolucci, F.; Paradisi, C.; Bignozzi, C. A.; Scandola, F. *J. Electroanal. Chem.* **1991**, *302*, 157.

orbitals of the dpp bridging ligands produced by the bischelation to two metal centers, indicate that the two one-electron peaks I and II of both complexes can be attributed to processes localized on the dpp bridging ligands (Figures 1a and 2a).

Peaks III and IV correspond to the exchange of two electrons each. The two two-electron peaks are separated from each other by 170 and 210 mV for $[(bpy)_2Ru(2,3-dpp)Ru(bpy)_2]^{4+}$ and $[(bpy)_2Ru(2,5-dpp)Ru(bpy)_2]^{4+}$, respectively. Such a separation is characteristic of the interaction between two electrons localized on two bpy's coordinated to the same Ru(II) center (∼200 mV), as observed in ruthenium mononuclear complexes containing two equivalent bpy's.[21−25] Accordingly, these processes are localized on the four terminal bpy ligands (Figures 1a and 2a). The separation between the two one-electron processes within each two-electron peak is larger than the statistical factor,[26a] which indicates the occurrence of electronic interactions between the two equivalent bpy's bound to different metal centers, mediated by the ruthenium atoms and the bridging ligand.[26b] For $[(bpy)_2Ru(2,3-dpp)Ru(bpy)_2]^{4+}$ the separation is larger, showing that the interaction between the redox centers is herein more effective than in $[(bpy)_2Ru(2,5-dpp)Ru(bpy)_2]^{4+}$.

The remaining part of the cvc's of both dinuclear species (peaks V and VI in Figures 1a and 2a) is made up of further four one-electron redox processes, similarly grouped as in peaks III and IV. The separation between the two groups of four one-electron processes (i.e., between peaks IV and V) is 580 and 640 mV for $[(bpy)_2Ru(2,3-dpp)Ru(bpy)_2]^{4+}$ and $[(bpy)_2Ru(2,5-dpp)Ru(bpy)_2]^{4+}$, respectively. Such values are those expected for the electronic pairing into the same molecular orbital, as found in the mononuclear bipyridyl Ru(II) complexes.[21−26] These last four one-electron processes therefore involve the same bpy-centered molecular orbitals also involved in peaks III and IV (Figures 1a and 2a).

The comparison of the redox series relative to the two dinuclear compounds shows that the first two one-electron voltammetric waves (peaks I and II) move toward less negative potentials on passing from $[(bpy)_2Ru(2,3-dpp)Ru(bpy)_2]^{4+}$ to $[(bpy)_2Ru(2,5-dpp)Ru(bpy)_2]^{4+}$. The remaining part of each redox series undergoes minor changes in the voltammetric pattern which correspond to noticeable shifts of the relative $E_{1/2}$ values, as a consequence of the different π-acceptor properties of the reduced bridging ligand and, mostly, of the different bridge-mediated electronic interactions among the terminal ligands. This contrasts with previous electrochemical studies[12] on the metal-centered oxidation processes of these complexes that showed that the two bridging ligands are indistinguishable as far as their electronic communication properties are concerned.

The electronic interaction between redox sites covalently linked by spacers in a multicomponent system is essentially promoted by the superexchange mechanism involving the spacer orbitals.[3a,27] One important factor for the entity of the super-exchange-mediated interaction is the energy gap between the orbitals in which reductions are localized (i.e., bpy-centered orbitals, in our case) and the LUMO of the bridge.

On the basis of preliminary semiempirical MO calculations (PM3 parametrization[28]), carried out on the free bridging ligands

with constrained dihedral angles so as to adopt the same conformation as in the dinuclear species,[29] no clear difference in the bridging-ligand-mediated interactions between reduced terminal ligands when 2,3-dpp is replaced by 2,5-dpp was expected. At this level of calculations, 2,3-dpp is electronically very similar to 2,5-dpp, the energy of the 2,3-dpp LUMO being about 10 meV higher than that of the 2,5-dpp one, and the succession of the unoccupied orbitals above the first LUMO is only slightly different for the two bridging ligands.

A better insight into the communication properties of the bridging ligand and, at the same time, support for the above localization of the redox processes were obtained by performing semiempirical calculations parametrized for transition metals (ZINDO−INDO/1[34]). The molecular structures of the two dinuclear species in their unreduced and reduced (up to the sixth reduction process) state have been optimized at the ZINDO level,[35] and the calculations were performed using the restricted open shell Hartree−Fock method for systems with unpaired electrons and the restricted Hartree−Fock one for those with closed shell electronic configuration.

The results of MO calculations carried out on the optimized molecular structures show that, in the unreduced state, the LUMO is centered on the bridging ligand. In agreement with the electrochemical results, the LUMO of the species with 2,5-dpp is at lower energy than that with 2,3-dpp. The second unoccupied MO also spans on the bridging ligand, while the successive four highest ligand-centered unoccupied MOs involve the four bpy ligands.

In the case of the one-electron-reduced state, the LUMO of the species with 2,3-dpp (formerly, the second unoccupied MO in the unreduced species) lies very close but lower (by ca. 0.3 eV) than the unoccupied MOs centered on the bpy's. On the contrary, in the case of the one-electron reduced complex with 2,5-dpp the second dpp-centered MO is higher in energy. This might suggest that, while for the latter spin-pairing takes place, a triplet state, with the two lowest dpp-centered virtual MOs singly occupied, is possible in the 2,3-dpp homologue. The energy gap existing between the singly occupied MO and the successive dpp-centered LUMO is however rather large, indicating that, also for the 2,3-dpp complex, spin-pairing occurs. In the doubly reduced complexes, the next four (unoccupied) MOs

(28) (a) Stewart, J. J. P. MOPAC Version 6.0. (b) Stewart, J. J. P. *J. Comput. Chem.* **1991**, *12*, 320.

(29) Whereas 2,5-dpp does not show any large conformational barrier, the 2,3-dpp ligand is hindered in position 3′ of each pyridyl ring, and for this reason it has to adopt different conformations depending on whether it is free,[30] monochelated as in the mononuclear species,[31,32] or bischelated as in the dinuclear ones.[32,33] In dinuclear complexes, 2,3-dpp should adopt a conformation as planar as possible to maximize the metal−ligand orbital overlapping. A certain degree of distortion from planarity (twisting of the pyrazine ring) is however expected, as also found in dinuclear rhenium(I) complexes with a 2,3-dpp bridging ligand[32] and in a dinuclear ruthenium-(II) species with 2,3-di(2-pyridyl)quinoxaline,[33] a bischelating ligand very similar to 2,3-dpp. These three different conformations of 2,3-dpp have expectedly different molecular orbital (MO) shapes and energies as shown by semiempirical MO calculations.[22]

(30) Huang, N. T.; Pennington, W. T.; Petersen, J. N. *Acta Crystallogr., Sect. C* **1991**, *47*, 2011.

(31) Belicchi Ferrari, M.; Gasparri Fava, G.; Pelosi, G.; Predieri, G.; Vignali, C.; Denti, G.; Serroni, S. *Inorg. Chim. Acta* **1998**, *275−276*, 320.

(32) Kirchhoff, J. R.; Kirschbaum, K. *Polyhedron* **1998**, *17*, 4033.

(33) Rillema, D. P.; Taghdiri, D. G.; Jones, D. S.; Keller, C. D.; Worl, L. A.; Meyer, T. J.; Levy, H. A. *Inorg. Chem.* **1987**, *26*, 578.

(34) (a) ZINDO program (developed by M. C. Zerner and co-workers, University of Florida) implemented on a CaChe Worksystem 3.11 (by the Oxford Molecular Group). (b) Bacon, A. D.; Zerner, M. C. *Theor. Chim. Acta* **1979**, *53*, 21. (c) Anderson, W. P.; Edwards, W. D.; Zerner, M. C. *Inorg. Chem.* **1986**, *25*, 2728.

(35) Anderson, W. P.; Cundary, T. R.; Drago, R. S.; Zerner, M. C. *Inorg. Chem.* **1990**, *29*, 1.

(24) Roffia, S.; Paradisi, C.; Bignozzi, C. A. In *Molecular Electrochemistry of Inorganic, Bioinorganic and Organometallic Compounds*; Pombeiro, A. J. L., McCleverty, J. A., Eds.; Kluwer Academic Publishers: Dordrecht, The Netherlands, 1993; p 217.

(25) Ohsawa, Y.; Hanck, K. W.; DeArmond, M. K. *J. Electroanal. Chem.* **1984**, *175*, 229.

(26) (a) Vlcek, A. A. *Coord. Chem. Rev.* **1982**, *43*, 39; *Rev. Chim. Min.* **1983**, *20*, 612. (b) Krejcik, M.; Vlcek, A. A. *Inorg. Chem.* **1992**, *31*, 2390.

(27) Giuffrida, G.; Campagna, S. *Coord. Chem. Rev.* **1994**, *135/136*, 517.
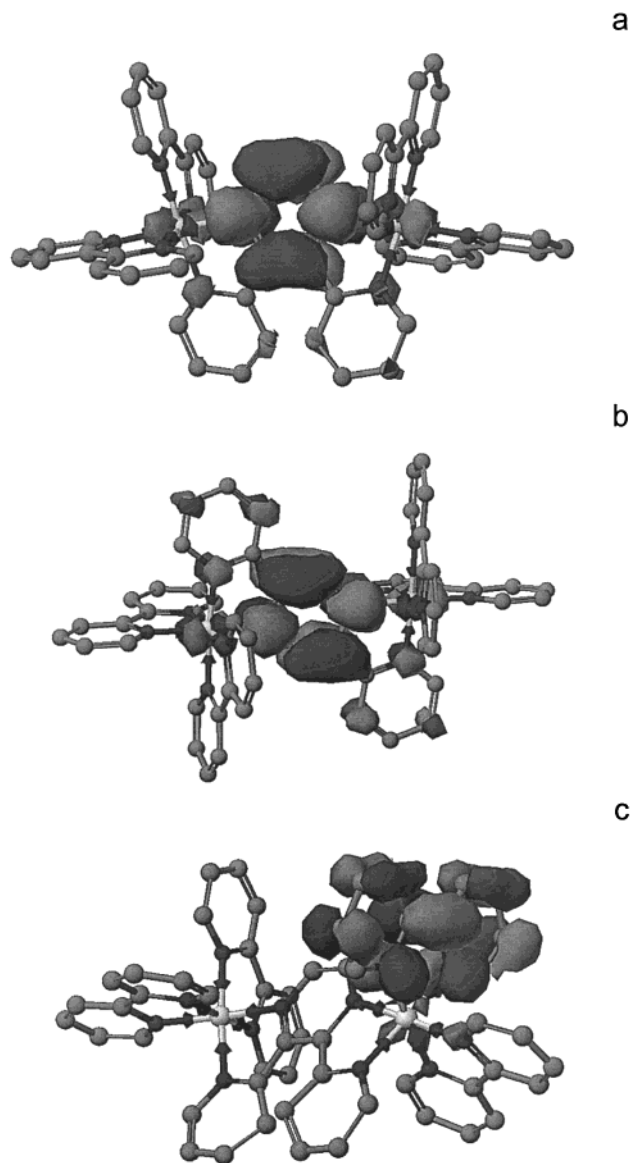
Figure 3. Molecular orbital surfaces showing the localization of relevant orbitals involved in the redox processes: (a) singly occupied MO of [(bpy)$_2$Ru(2,3-dpp)Ru(bpy)$_2$]$^{3+}$ (one-electron-reduced species) centered on the 2,3-dpp bridging ligand; (b) singly occupied MO of [(bpy)$_2$Ru(2,5-dpp)Ru(bpy)$_2$]$^{3+}$ (one-electron-reduced species) centered on the 2,5-dpp bridging ligand; (c) singly occupied MO of [(bpy)$_2$Ru-(2,3-dpp)Ru(bpy)$_2$]$^+$ (triply one-electron-reduced species) centered on a terminal bpy ligand.

are centered on the bpy's and the successive ligand-centered unoccupied MO involves the bridging ligand.

Incidentally, the molecular geometry optimization of the doubly reduced (singlet state) dinuclear species shows that the C−C bond length between pyrazine and pyridine rings in the bridging ligands decreases (from 1.46 to 1.39 and 1.43 Å for 2,3-dpp and 2,5-dpp, respectively), because of an increase of the C−C bond order in the 2−2′, 3−2″ (2,3-dpp) and 2−2′, 5−2″ (2,5-dpp) positions (see Figure 3a,b). This means that, in the 2,3-dpp-bridged species, the addition of two electrons constrains the bridge to an even more planar conformation than in the unreduced complex. The geometry optimization of the two species for the successive four reductions, under the hypothesis that all the added electrons are unpaired (since the virtual bpy-centered MOs are closely spaced), shows a shortening of the C−C bond in position 2−2′ of reduced bipyridyls (Figure 3c). The C−C bond length changes from 1.46 Å for
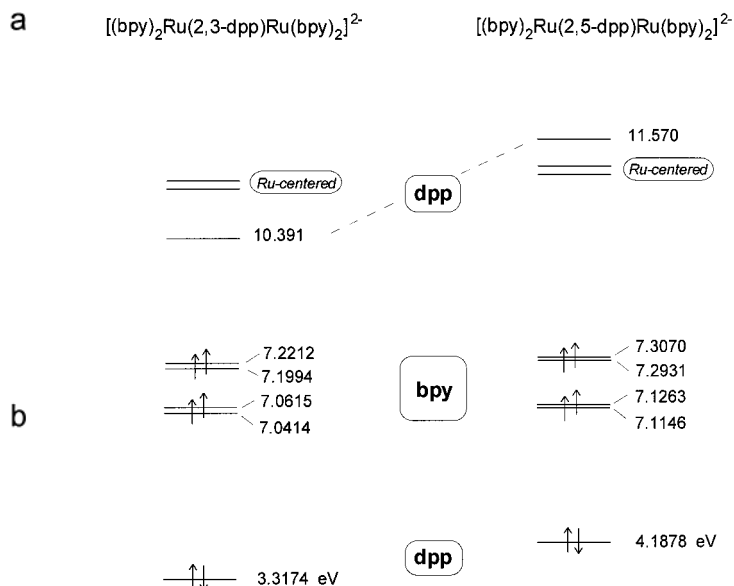

Figure 4. Energy diagrams of MOs obtained for the [(bpy)$_2$Ru(2,3-dpp)Ru(bpy)$_2$]$^{2-}$ and [(bpy)$_2$Ru(2,5-dpp)Ru(bpy)$_2$]$^{2-}$ compounds considering the first two one-electron reductions as coupling into the same orbital and the successive four processes as unpaired electrons.

the unreduced bpy to 1.42 Å after reduction. This is also found to happen for the first reduction of free bpy, as experimentally observed by resolving the X-ray crystal structure of the doubly reduced product of a bypiridyl Ru(II) mononuclear complex.[18]

The comparison of the energy diagrams of MOs involved in the four bpy-centered redox processes for the two dinuclear species shows several important features which are in good agreement with the electrochemical results, as shown in Figure 4 for the six-electron-reduced species. In particular, the energy difference between two MOs localized onto bpy's bound to different metal centers (i.e., corresponding to processes comprised in peaks III and IV of cvc's, Figures 1a and 2a) is larger in the case of the 2,3-dpp than of the 2,5-dpp bridging ligand, in agreement with the voltammetric results. Vice versa, the separation between the couple of two closely spaced MOs, centered onto bipyridyl coordinated to the same metal atom, is larger for the species with 2,5-dpp than in the complex with the 2,3-dpp bridging ligand, and this is also in agreement with the voltammetric results. Moreover, again reproducing the experimental findings, (i) the bpy-centered MOs of the dinuclear species with 2,3-dpp are at lower energy (i.e., easier to reduce) than the corresponding ones in the species containing 2,5-dpp and (ii) a lower spin-pairing energy on the dpp-centered MO results from the calculations for the 2,3-dpp species with respect to the 2,5-dpp one. Finally, within a superexchange model for the interaction between remote (bpy-centered) redox sites in the doubly reduced complexes, calculations indicate that 2,3-dpp is expectedly a better mediator, possessing a local unoccupied MO at lower energies than that of the 2,5-isomer (Figure 4).

Trinuclear Complexes. The species [{(bpy)$_2$Ru(2,3-dpp)}$_2$Ru-(bpy)]$^{6+}$ and [{(bpy)$_2$Ru(2,5-dpp)}$_2$Ru(bpy)]$^{6+}$ (Chart 1) have been studied. The voltammetric behavior has been investigated in DMF at low and room temperature, and the corresponding cvc's recorded at 0.05 V/s and −54 °C are shown in Figures 5a and 6a. Both species show redox series made up of fourteen successive one-electron reduction processes, which are grouped in six multielectron voltammetric peaks, labeled by Roman numbers I−VI. The voltammetric peaks I and II are both made up of two one-electron reductions, peaks III and IV contain two
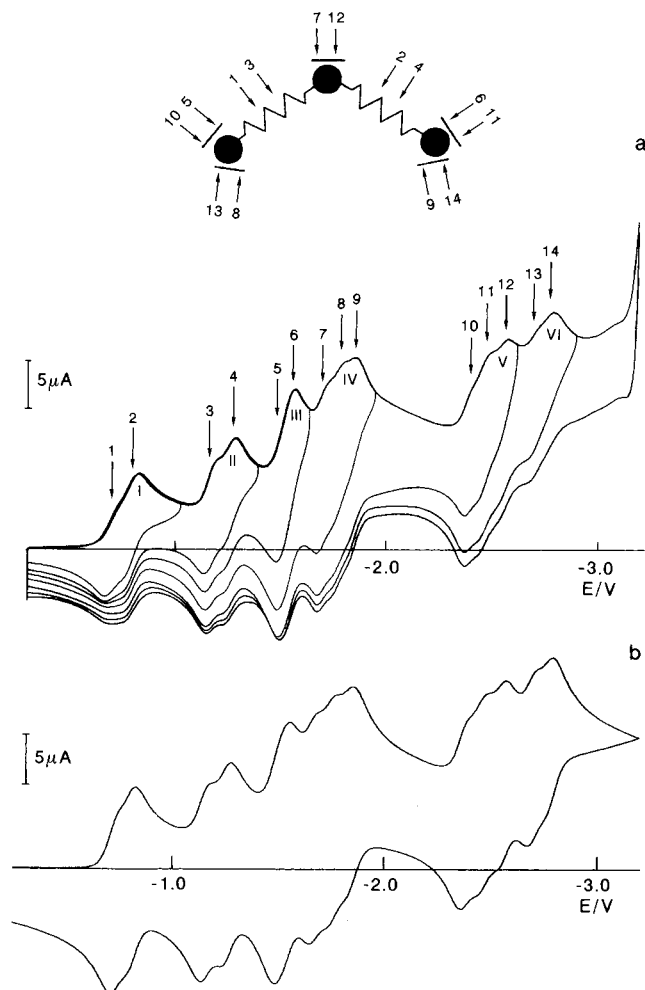
Figure 5. (a) Cyclic voltammetric curves for a 0.5 mM [{(bpy)$_2$Ru-(2,3-dpp)}$_2$Ru(bpy)]$^{6+}$, 0.05 M TEATFB/DMF solution. Working electrode Pt; $T = -54$ °C; scan rate 0.05 V/s. The proposed localization of the redox processes is indicated. (b) Simulated cyclic voltammetric curve for the species [{(bpy)$_2$Ru(2,3-dpp)}$_2$Ru(bpy)]$^{6+}$ under the conditions of (a).

Figure 6. (a) Cyclic voltammetric curves for a 0.5 mM [{(bpy)$_2$Ru-(2,5-dpp)}$_2$Ru(bpy)]$^{6+}$, 0.05 M TEATFB/DMF solution. Working electrode Pt; $T = -54$ °C; scan rate 0.05 V/s. The proposed localization of the redox processes is indicated. (b) Simulated cyclic voltammetric curve for the species [{(bpy)$_2$Ru(2,5-dpp)}$_2$Ru(bpy)]$^{6+}$ under the conditions of (a).

and three one-electron processes, respectively, and finally peaks V and VI are formed by three and two one-electron reductions, respectively. The number of electrons exchanged in each voltammetric peak has been confirmed by voltammetry at a solid electrode with periodical renewal of the diffusion layer (see the Supporting Information), steady-state voltammetry at ultramicroelectrodes, and digital simulation of the voltammetric curves. In the simulations, it has been assumed that all processes were electrochemically and chemically reversible. This is certainly an acceptable assumption as far as the first groups of reductions (i.e., up to peak V) are concerned, while some chemical irreversibility (EC mechanism) should be introduced in the simulation of the last processes. Evidence of chemical instability of the highest members of the redox series is, for instance, the lower height generally observed for the corresponding reoxidation peaks with respect to the reduction ones. This is also observed in the case of tetra- and hexanuclear complexes (vide infra), and it is likely associated with either the high charge of the electrogenerated anions or interaction with the solvent, considering that these reductions are located at potentials where degradation of the latter can occur. For the sake of simplicity, the chemical reversibility approximation was however adopted in the simulations. Implicitly, this means that the $E_{1/2}$ values relative to the last processes, given in Table 1, are affected by a greater uncertainty than those relative to the previous ones.
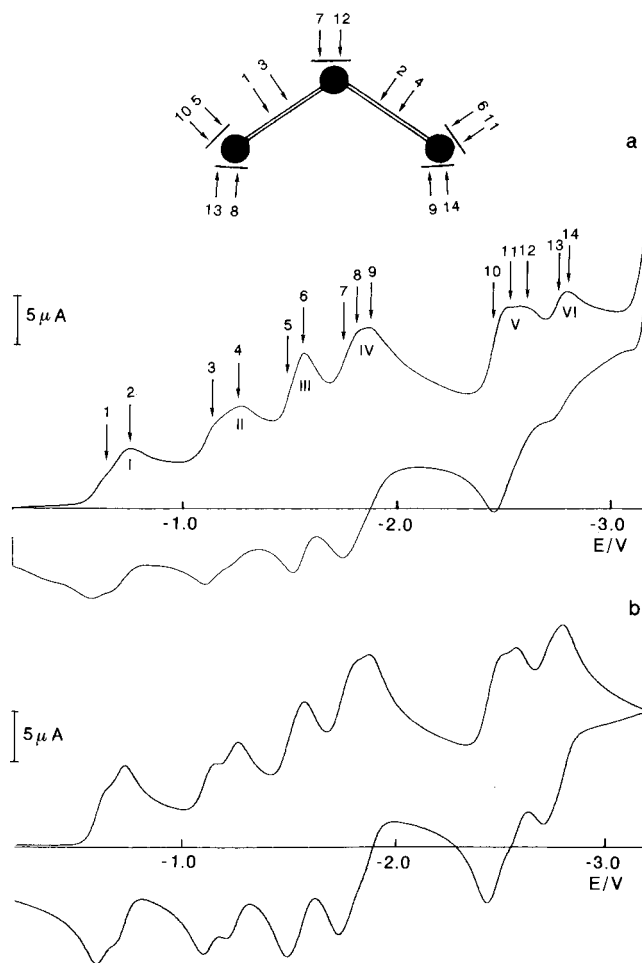
The result of the simulation is reported in Figures 5b and 6b and shows a rather good agreement with the experimental curves.

Similarly to what happens for the dinuclear complexes, a noteworthy resemblance of the voltammetric patterns is observed between the two trinuclear species. Again, the main differences existing between the corresponding cvc's are (i) peaks I and II are at less negative potentials in the case of the 2,5-dpp-bridged ligand and (ii) the processes occurring at the bpy centers bound to adjacent metal centers (i.e., the redox processes in peaks IV and V) are differently spaced depending on the type of bridging ligand.

Localization of Redox Sites and Their Mutual Interactions in Trinuclear Complexes. The maximum extension of the cathodic redox series for the trinuclear species, expected on the basis of the electrochemical behavior of terminal and bridging ligands, is 14 processes, in agreement with the experimental results. On the basis of the electrochemical behavior of free ligands, mononuclear building moieties, and dinuclear species, the four reductions in the voltammetric peaks I and II involve in both complexes the two bridging ligands. The separation between the voltammetric peaks I and II (i.e., the separation between the second and the third reductions) is of the same magnitude as that in the corresponding dinuclear species and is related to the electron pairing into the same redox dpp orbital.

The voltammetric peaks III and IV in both complexes are made up of two and three reduction processes, respectively. These two peaks resemble peaks III and IV of the corresponding dinuclear species, apart from the number of electrons involved which corresponds to the number of bpy ligands present in the molecule (five), and are reasonably assigned to the first reductions of the terminal ligands. The fact that in the case of the trinuclear species the separation between peaks III and IV is somewhat smaller than in the corresponding dinuclear species (see also Table 1) is explained by localizing the first reduction in peak IV on the bpy of the central ruthenium ion, which is absent in the case of dinuclear species, thus shrinking the gap between the two doublets relative to the peripheral units.[36]

In the remaining part of the cvc's, two voltammetric peaks, V and VI, are observed which comprise three and two closely spaced one-electron processes, respectively. The separation between peaks IV and V is close to 0.6 V, indicating that the last five processes (in peaks V and VI) correspond to the second reduction localized onto the five bpy centers.

The localizations of the various reductions for the trinuclear complexes $[\{(bpy)_2Ru(2,3\text{-}dpp)\}_2Ru(bpy)]^{6+}$ and $[\{(bpy)_2Ru(2,5\text{-}dpp)\}_2Ru(bpy)]^{6+}$ are shown in Figures 5a and 6a, respectively.

Higher Nuclearity Complexes. Tetranuclear Complex. The electrochemistry of the tetranuclear species $[\{(bpy)_2Ru(2,3\text{-}dpp)\}_3Ru]^{8+}$ has been investigated in DMF at both room and low temperature. Its cvc recorded at -54 °C and a sweep rate of 0.05 V/s is reported in Figure 7a. As expected, the cvc consists of eighteen successive one-electron reduction processes grouped in six three-electron voltammetric peaks, labeled as I–VI. Figure 7b shows the simulated cvc, calculated assuming all the processes as electrochemically and chemically reversible, which is in rather good agreement with the experimental curve. Considerations analogous to those for the trinuclear complexes can be made as far as the chemical stability of the highest members of the redox series is concerned. The $E_{1/2}$ values for each redox process, obtained from the digital simulation, are collected in Table 1.

As for the localization of the various processes and the mutual interactions between the redox sites, notice that the tetranuclear complex can be naively regarded as an "electronically symmetric" species made up of a central ruthenium core with a first ligand shell of bridging ligands and a second ligand shell constituted by bpy's. Since 2,3-dpp is easier to reduce than bpy,[21] the six one-electron reductions in peaks I and II are localized on the three bridges, whereas the remaining twelve one-electron processes (peaks III–VI) are mainly localized on the six bpy's. The morphology of the voltammetric curve resembles those of the corresponding dinuclear and trinuclear species. In particular, the I–II peak separation and that between peaks IV and V are about 0.34 and 0.6 V, respectively. These two values represent the electron pairing energy on the 2,3-dpp and bipyridyl molecular orbitals, respectively, as observed in the species having lower nuclearity. The localizations of the various reduction processes are shown in Figure 7a.

Hexanuclear Complex. The hexanuclear species $[\{(bpy)_2Ru(2,3\text{-}dpp)\}_2Ru(2,3\text{-}dpp)Ru\{(2,3\text{-}dpp)Ru(bpy)_2\}_2]^{12+}$ is that with the highest nuclearity investigated in this work. In Figure

(36) Interestingly, in agreement with such a localization of the seventh reduction in both trinuclear complexes, the homologue complex $[\{(bpy)_2Ru(2,3\text{-}dpp)\}_2Ru(biq)]^{6+}$, bearing a 2,2′-biquinoline (biq) ligand instead of bpy in the central unit (Chart 1), shows a strikingly similar CV behavior, but by contrast to the species considered in this work, peaks III and IV are both two-electron peaks, the missing reduction process, clearly involving the biq ligand, being shifted to more cathodic potentials.

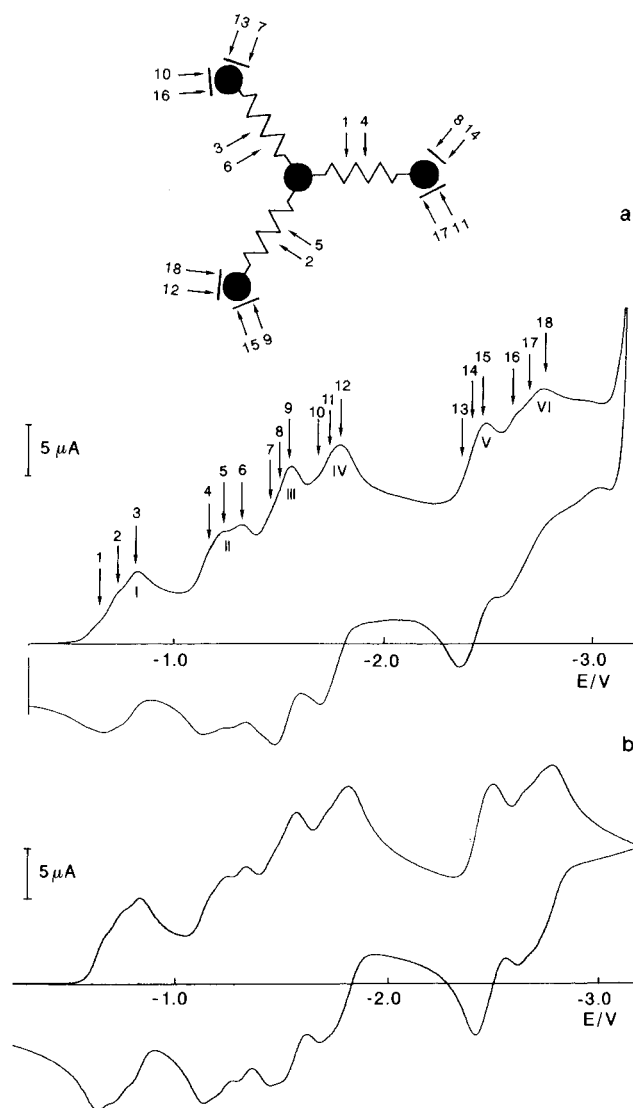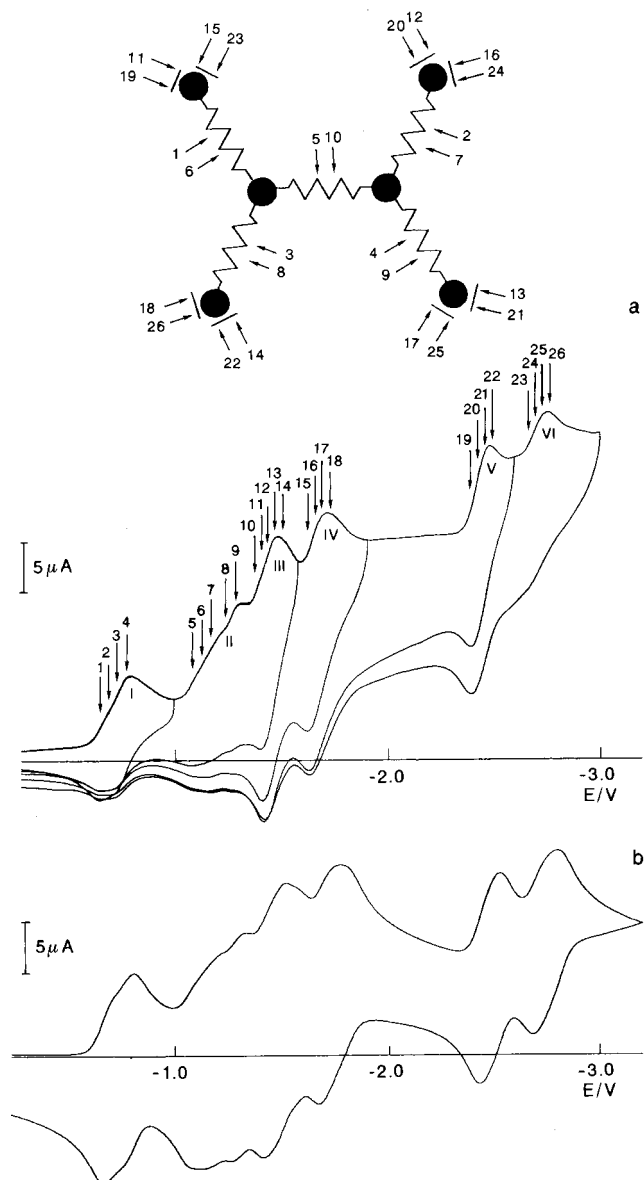**Figure 7.** (a) Cyclic voltammetric curves for a 0.5 mM $[\{(bpy)_2Ru(2,3\text{-}dpp)\}_3Ru]^{8+}$, 0.05 M TEATFB/DMF solution. Working electrode Pt; $T = -54$ °C; scan rate 0.05 V/s. The proposed localization of the redox processes is indicated. (b) Simulated cyclic voltammetric curve for the species $[\{(bpy)_2Ru(2,3\text{-}dpp)\}_3Ru]^{8+}$ under the conditions of (a).

8a the cvc recorded at -55 °C and 0.05 V/s is reported. A total number of twenty-six successive one-electron redox processes grouped into six multielectron peaks (I–VI) are observed. Peaks I, IV, V, and VI are made up of four one-electron closely spaced redox processes, while peaks II and III contain five one-electron reductions each. The number of electrons exchanged in each voltammetric peak has been determined as described for the other polynuclear species (see also the Supporting Information), and the digital simulation of the cvc, shown in Figure 8b, is in fairly good agreement with the experimental one. The comparison between the experimental and simulated cvc's indicates that, as reported above for both the tri- and tetranuclear species, slow irreversible chemical reactions are coupled to the last redox processes (those comprised in peak VI). The $E_{1/2}$ potentials for each redox process, determined by simulation of the experimental cvc, are collected in Table 1.

The experimental ligand-based redox series for this species (26 processes) is coincident with the maximum number of reductions expected on the basis of the electrochemical behavior

Figure 8. (a) Cyclic voltammetric curves for a 0.5 mM [{(bpy)$_2$-Ru(2,3-dpp)}$_2$Ru(2,3-dpp)Ru{(2,3-dpp)Ru(bpy)$_2$}$_2$]$^{12+}$, 0.05 M TEATFB/DMF solution. Working electrode Pt; $T = -55$ °C; scan rate 0.05 V/s. The proposed localization of the redox processes is indicated. (b) Simulated cyclic voltammetric curve for the species [{(bpy)$_2$Ru(2,3-dpp)}$_2$Ru(2,3-dpp)Ru{(2,3-dpp)Ru(bpy)$_2$}$_2$]$^{12+}$ under the conditions of (a).

of the free and chelated ligands. Concerning the localization of the various processes and their mutual interactions, it should be noticed that the hexanuclear species is made of two trinuclear moieties connected by a 2,3-dpp briding ligand (see Figure 8a). In other words, the electrochemical behavior should be similar to that observed for the trinuclear species with 2,3-dpp bridges. Comparison of the cvc of the hexanuclear complex with that of the trinuclear species with the 2,3-dpp bridging ligands suggests that the four processes in peak I are localized on the four "external" 2,3-dpp ligands, since the interactions between redox centers destabilize the ligands bound to the same metal center. The first out of the five processes comprised in peak II is localized on the "central" 2,3-dpp, because the separation between peaks I and II is unusually small. The other four processes in peak II represent the electron pairing into the same redox orbital of "external" 2,3-dpp. The first process contained in peak III instead corresponds to the electron pairing for the

central bridging ligand. The remaining four processes of peak III and those in peak IV are the first reduction of the eight bpy's, and the last two voltammetric peaks (V and VI) comprise the second reduction of the same ligands. The separation of about 0.6 V between peaks IV and V confirms this assignment.

Spectroelectrochemistry. UV/vis/near-IR spectroelectrochemistry is a very powerful tool for the characterization of the redox orbitals of Ru(II) polypyridyl complexes.[37−39] In the framework of the localized MO model, the spectroelectrochemical investigation of these species allows us to gain further support for the attribution of the various redox processes.

Only the spectroelectrochemistry of the dinuclear species [(bpy)$_2$Ru(2,3-dpp)Ru(bpy)$_2$]$^{4+}$ has been studied, since such a complex is an adequate model for 2,3-dpp-bridged polynuclear species with higher nuclearity. The investigation has been carried out in the 255−1650 nm wavelength range, and it concerns the first six reduction processes, under experimental conditions very similar to those used for the voltammetric studies (DMF and aprotic conditions). Previous investigations, only for the first four reductions and in a more limited spectral range (350−800 nm), have been reported.[39,40]

The chemical stability of the various reduction products was checked by recovering the spectrum of the original unreduced species at the starting potential (i.e., 0.0 V vs Ag/AgCl), after each experiment. Moreover, the appearance of clean and stable isosbestic points during the whole experiment is evidence of the chemical reversibility of the process. Finally, the voltammetry with periodical renewal of the diffusion layer (shown in Figures 1b and 2b) also gives a good indication about the stability of the various electrogenerated products on a time scale longer than that of cyclic voltammetry.

The spectrum of the dinuclear complex, shown in Figure 9 (curve a), is dominated in the UV region by the very intense absorption peak with a maximum at 34 800 cm^{-1} and a shoulder around 30 000 cm^{-1}. In the remaining part of the spectrum, two bands can be observed in the visible region, at 23 200 and 19 000 cm^{-1} (the relatively weak absorptions in the near-IR are due to the background electrolyte). As already known, the absorptions in the UV region are due to bpy and 2,3-dpp intraligand transitions, respectively, at 34 800 and 30 000 cm^{-1}, while the two bands in the visible region are due to metal-to-ligand charge-transfer transitions, Ru(II) → bpy and Ru(II) → 2,3-dpp, respectively.

The spectrum of the first reduction product, recorded at −32 °C in DMF and reported in Figure 9 (curve b), shows the disappearance of the 2,3-dpp intraligand and the Ru(II) → 2,3-dpp bands, and the appearance of a new band around 19 800 cm^{-1} which can be attributed to the Ru(II) → bpy charge-transfer transitions, shifted to lower energies with respect to the unreduced species. A possible contribution from a $\pi-\pi^*$ transition of the bischelated 2,3-dpp ligand radical anion can also occur.

The second reduction produces spectral changes which support its assignment as an electron pairing on the 2,3-dpp bridging ligand. An increase of the band around 19 800 cm^{-1} can be observed (Figure 9, curve c) and a new band appears around 29 500 cm^{-1}, which may be attributed to a (2,3-dpp)$^{2-}$ → Ru(II) charge-transfer transition. It can also be noted that

(37) Gale, R. J., Ed. *Spectroelectrochemistry. Theory and Practice*; Plenum Press: New York, 1988.

(38) Heath, G. A.; Yellowlees, L. J.; Braterman, P. S. *J. Chem. Soc., Chem. Commun.* **1981**, 287.

(39) Berger, R. M. *Inorg. Chem.* **1990**, *29*, 1920.

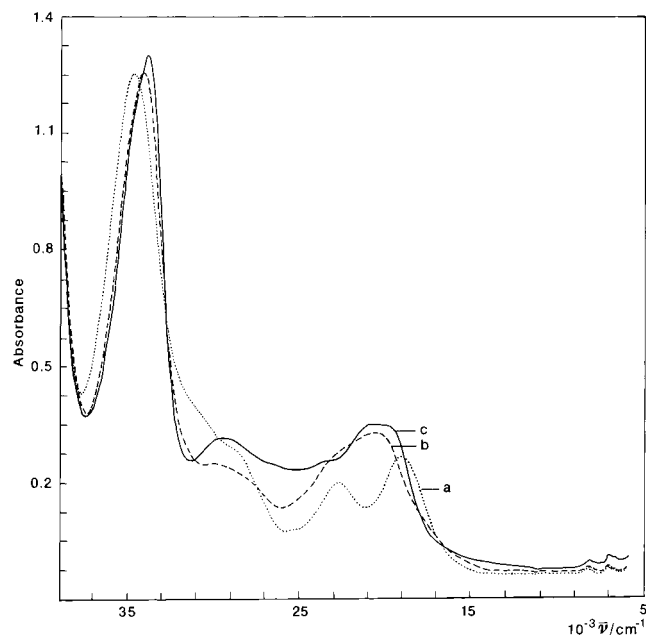(40) Cooper, J. B.; MacQueen, D. B.; Petersen, J. B.; Wertz, D. W. *Inorg. Chem.* **1990**, *29*, 3701.

Figure 9. UV/vis/near-IR spectroelectrochemistry of a 0.55 mM [(bpy)$_2$Ru(2,3-dpp)Ru(bpy)$_2$]$^{n+}$, 0.1 M TBATFB/DMF solution, $T = -32$ °C: (a) $n = 4$, absorption spectrum of the unreduced species at $E = 0$ V (vs Ag/AgCl); (b) $n = 3$, first reduction steady spectrum at $E = -0.82$ V (vs Ag/AgCl); (c) $n = 2$, second reduction steady spectrum at $E = -1.20$ V (vs Ag/AgCl).

Figure 10. UV/vis/near-IR spectroelectrochemistry of a 0.55 mM [(bpy)$_2$Ru(2,3-dpp)Ru(bpy)$_2$]$^{n+}$, 0.1 M TBATFB/DMF solution, $T = -32$ °C: (c) $n = 2$, second reduction steady spectrum at $E = -1.20$ V (vs Ag/AgCl); (d) $n = 0$, fourth reduction steady spectrum at $E = -1.56$ V (vs Ag/AgCl); (e) $n = -1$, fifth reduction steady spectrum at $E = -1.70$ V (vs Ag/AgCl); (f) $n = -2$, sixth reduction steady spectrum at $E = -1.85$ V (vs Ag/AgCl).

the first and second reduction processes cause a red shift of the bpy intraligand transition, without any significant decrease of its intensity. These results confirm that the first two processes do not concern the bpy ligands. The red shift of the bipyridine intraligand bands can be attributed to an electronic destabilization of the corresponding HOMOs of the bpy's, as a consequence of the two electrons introduced onto the bridging ligand redox orbital.

The examination of the spectra corresponding to the reductions from the third to the sixth one (reported in Figure 10 (curves d, e, and f)) shows a stepwise decrease of the π−π* bpy intraligand band until its complete disappearance. The bands observed in the 30 000 cm^{-1} region can be attributed to π−π* intraligand transitions of the one-electron-reduced bpy's since they look like those of [Ru(bpy)$_3$]$^-$ (i.e., triply reduced [Ru(bpy)$_3$]$^{2+}$).[38] It is therefore possible to say that these last four one-electron reduction processes are centered on the four terminal ligands. This represents a definitive confirmation of the attribution based on voltammetric arguments.

Conclusions

The electrochemical behavior of a family of polynuclear bipyridine-type ruthenium(II) complexes having general formula [Ru$_n$(bpy)$_{n+2}$(2,X-dpp)$_{n-1}$]$^{2n+}$ (with $n = 2$, 3, 4, and 6, X = 3 or 5, dpp = bis(2-pyridyl)pirazine, and bpy = 2,2'-bipyridine) has been studied in DMF under strictly aprotic conditions to have a potential window as wide as possible, and to avoid any nonintrinsic reactivity of the electrodically generated species.

The cathodic redox series of the investigated compounds are made up of 10, 14, 18, and 26 reversible one-electron processes for dinuclear, trinuclear, tetranuclear, and hexanuclear species, respectively. Such redox series are the largest ones so far observed for this kind of complex and, to the best of our knowledge, for well-defined supramolecular systems. The observed processes are reversible both in CV and on longer time scales. For all the complexes investigated the first ligands
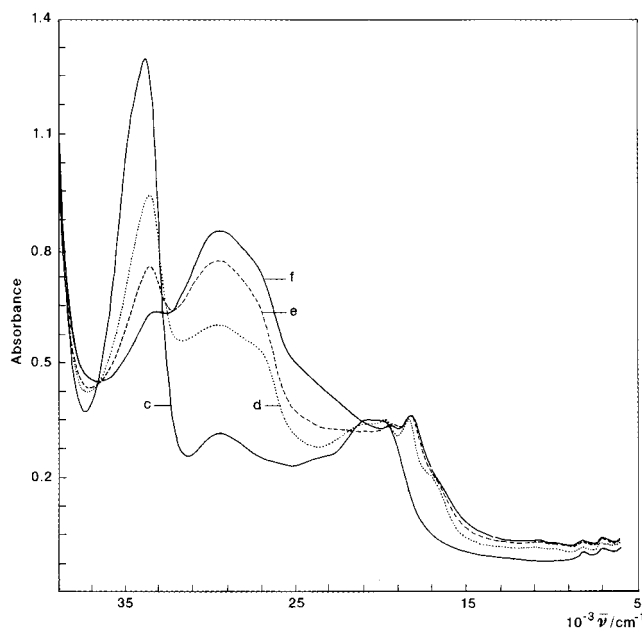
to be reduced are the bridging ones, mainly as a consequence of the great stabilization of their redox orbitals caused by the bischelation. The terminal ligands begin to be reduced only when the bridges are electronically saturated.

The digital simulation of the voltammetric curves was a fundamental tool to determine most of the standard potentials and to evaluate the mutual interactions among the various redox centers. The knowledge of the redox behavior of the free ligands and that of the mononuclear building blocks and the changes of the voltammetric pattern as a consequence of replacing one ligand (bridging and/or terminal) with another one in the same complex have allowed us to assign the localization of each redox process. Spectroelectrochemical experiments carried out at low temperature on [(bpy)$_2$Ru(2,3-dpp)Ru(bpy)$_2$]$^{4+}$, which can be considered as a model for all other polynuclear complexes with the same type of bridge, and semiempirical calculations (ZINDO) carried out on the [(bpy)$_2$Ru(2,X-dpp)Ru(bpy)$_2$]$^{4+}$ (X = 3 or 5) compounds have confirmed the assignments concerning the localization of the various redox processes.

Despite the increase of the nuclearity and, as a consequence, of the number of redox processes, it is always possible to distinguish two regions in the voltammetric curves of the tetranuclear and hexanuclear complexes, as happens for the dinuclear ones. In the first part of the cvc's there are bridging ligand reductions, and in the second one those of the terminal ligands. In other words, the increase of the number of redox steps with the growth of nuclearity (i.e., of molecular dimension) does not modify the mutual interactions among the redox centers because the processes are localized, and therefore, the average local electronic density remains constant along the whole series of polynuclear species.

Supporting Information Available: Steady-state-like voltammetric curves, obtained with periodical renewal of the diffusion layer at the Pt electrode, for tri-, tetra- and hexanuclear species (PDF). This material is available free of charge via the Internet at http://pubs.acs.org.

JA9916456